Brain Imaging and Behavior (2019) 13:75–86
https://doi.org/10.1007/s11682-017-9803-y

ORIGINAL RESEARCH

rCBF and cognitive impairment changes assessed by SPECT and ADAS-cog in late-onset Alzheimer's disease after 18 months of treatment with the cholinesterase inhibitors donepezil or galantamine

Yukihiko Shirayama[1] · Michio Takahashi[1] · Yasunori Oda[2] · Kouhei Yoshino[1,2] · Koichi Sato[1] · Toshiyuki Okubo[3] · Masaomi Iyo[2]

Published online: 15 December 2017
© Springer Science+Business Media, LLC, part of Springer Nature 2017

Abstract
Late-onset Alzheimer's disease (AD) differs substantially from early-onset AD. In this cross sectional study we investigated brain perfusion changes after 18 months of treatment with cholinesterase inhibitors (ChEIs) donepezil or galantamine. Twenty-five drug-naïve late-onset AD patients were recruited from outpatient clinics. We examined brain perfusion using single photon emission computed tomography (SPECT) and used three-dimensional stereotactic surface projection (3D-SSP) and the stereotactic extraction estimation method (SEE) level 3 to analyze classified gyrus level segments. We assessed cognitive function using the Alzheimer's Disease Assessment Scale-cognitive subscale (ADAS-cog) grouped into three subgroup domains, language, memory, and praxis. In the follow-up data, some regions were further hypoperfused, reflecting worsening of the disease, while other regions showed alleviated hypoperfusion, potentially related to the ChEIs treatment. Regional cerebral blood flow (rCBF) decreased in the parietal cortex and increased in the frontal and the limbic cortices. Increased hypoperfusion significantly correlated with ADAS-cog scores changes were seen in the superior parietal lobule, inferior parietal lobule, angular gyrus, and supramarginal gyrus of the parietal cortex. Alleviated hypoperfusion significantly related to recovery of ADAS-cog scores were seen in the rectal and paracentral lobule of the frontal cortex, and the anterior cingulate of the limbic cortex. These regions showed significant relationships with total ADAS-cog and language, memory and praxis subscales scores. The current longitudinal study indicates prominent rCBF changes and their relationships with changes in ADAS-cog scores in late-onset AD patients.

Keywords SPECT · Late-onset · Alzheimer's disease · ADAS-cog

Introduction

Single-photon emission computed tomography (SPECT) studies show perfusion reduction associated with Alzheimer's disease (AD) in the parieto-temporal association cortices early in the disease process, and in the frontal association cortex in the advanced disease state (Kumar et al. 1991; Waldemar et al. 1994). Longitudinal SPECT evaluation of mild AD showed decreased perfusion in the anterior thalamus, anterior cingulate and posterior cingulate gyrus (Johnson et al. 1998). Another SPECT study showed a significant regional cerebral blood flow (rCBF) decline in the middle frontal gyri, inferior parietal lobe, inferior temporal gyri, middle and inferior occipital gyri, and hippocampus in early AD (Kogure et al. 2000). Notably, hypoperfusion could be associated with neuronal degeneration, and it is well known that cholinesterase inhibitors (ChEIs) including donepezil and galantamine increased rCBF in the brains of AD patients (Nakano et al. 2001; Ushijima et al. 2006; Keller et al. 2011).

Recent studies have shown differences between late and early-onset AD. Patients who develop the disease after age 65 (late-onset) show topographic patterns of brain gray matter atrophy in the medial temporal lobe as well as hippocampal atrophy while early-onset AD shows atrophy in

✉ Yukihiko Shirayama
shirayama@rapid.ocn.ne.jp

[1] Department of Psychiatry, Teikyo University Chiba Medical Center, 3426-3 Anesaki, Ichihara 299-0111, Japan

[2] Department of Psychiatry, Chiba University Graduate School of Medicine, Chiba, Japan

[3] Department of Radiology, Teikyo University Chiba Medical Center, Ichihara, Japan

the occipital and parietal lobes including precuneus (Ishii et al. 2005; Frisoni et al. 2007; Möller et al. 2013; Cavedo et al. 2014). Furthermore, early and late-onset AD show distinct paterns of memory impairment (Joubert et al. 2016). Late-onset AD patients also show selective parahippocampal white matter loss relative to ealy-onset AD patients (Canu et al. 2012), but the pathogenic mechanism of late-onset AD remains unclear.

A SPECT study showed a relationship between late-onset AD and hypoperfusion in the medial temporal lobe and hippocampal regions, while patients with early-onset AD exhibited a greater rCBF decrease in the posterior cortical association area (Kemp et al. 2003). Our recent study demonstrated a reduction of rCBF in the frontal, temporal and limbic lobe relative to that seen in the parietal and occipital lobe in late-onset AD patients (Takahashi et al. 2017). Perturbed rCBF may contribute to the pathogenesis of late onset AD.

The well-documented typical AD course begins with episodic memory dysfunction followed by additional cognitive impairment (Mckhann et al. 1984; Dubois et al. 2010). Late-onset AD patients show strong cognitive deficits in memory, moderate deficits for language, and weak deficits in praxis (Grady et al. 1987, Sá et al. 2012). Furthermore, late-onset AD patients with greater hypometabolism in inferior fronto-temporal regions have verbal memory deficits (Kaiser et al. 2012). Cognitive function was examined using the Alzheimer's Disease Assessment Scale cognitive subscale (ADAS-cog) with further subscales grouped into the domains language, memory, and praxis. We recently demonstrated that hypoperfusion in the cingulate and parahippocampal gyrus of the limbic lobe were significantly correlated with ADAS-cog memory subscale scores in late-onset AD (Takahashi et al. 2017).

Since early onset AD is a progressive neurodegenerative disorder, it is likely that late-onset AD is also a progressive disease characterized by increasing cognitive decline. However, the time course of hypoperfusion and cognitive dysfunction in late onset AD and the effects of ChEIs treatment remain unknown. Repeated rCBF measurement is supposed to be an objective maker of disease progression. We hypothesize that increases in rCBF reduction z scores are related to increased cognitive dysfunction, while decreases in rCBF reduction z scores are associated with the improvement of that dysfunction. Here we examine brain perfusion by SPECT and longitudinal changes in cognitive deficits by ADAS-cog from baseline to follow up at 18 months with the ChEI treatments donepezil and galantamine in late-onset AD patients. We analyzed brain perfusion using three dimensional stereotactic surface projection (3D-SSP) and the stereotactic extraction estimation method (SEE) level 3.

Materials and methods

Participants

Twenty-five late-onsest drug-naïve AD patients were enrolled from the outpatient clinic of Teikyo University Chiba Medical Center (Table 1). AD diagnosis was in accordance with the DSM-IV-TR criteria for Alzheimer's type dementia (American Psychiatric Association 1994), and all AD patients fulfilled the National Institute of Neurological and Communicative Disorders and Stroke and the Alzheimer's Disease and Related Disorders Association (NINCDS-ADRDA) criteria for probable or possible AD (McKhann et al. 1984). MMSE scores were required to be below 26, and MRI or CT was performed when needed (in cases of normal pressure hydrocephalus, for example). Hypothyroidism was ruled out by verification of thyroid function and vitamin levels. Other types of dementia such as vascular dementia, frontotemporal dementia and dementia with lewy bodies were excluded. Since ChEIs significantly influence rCBF and cognitive function in AD patients (Li et al. 2012), patients were not currently receiving treatment

Table 1 Demographic characteristics

	At baseline	Follow up 1.5 year	p-value
Age (y)	77.0 ± 6.4		
Sex (M/F)	5 / 20		
HIS	2.7 ± 2.1		
Below 4 (n)	20		
Above 5 (n)	5		
Hypertension (n)	6		
Hyperlipidemia (n)	3		
Diabetes mellitus (n)	4		
MMSE	20.3 ± 3.6		
ADAS-cog total	18.38 ± 6.13	19.32 ± 8.39	0.465
ADAS-cog language	2.60 ± 2.10	2.60 ± 2.91	1.000
ADAS-cog memory	12.54 ± 4.43	13.38 ± 4.37	0.261
ADAS-cog Praxis	3.44 ± 2.06	3.24 ± 2.20	0.684
Clinical outcome by ADAS-cog total (n)			
Worsen (plus 3)		6 (24%)	
Recover (minus 3)		7 (28%)	
Maintain		12 (48%)	
Drugs (n)			
Donepezil (5 mg/day)		18	
Galantamine (16 mg/day)		7	

Deta are shown in mean ± SD

Statistical result of comparison between the below 4 and above 5 groups on the HIS using Student's t-test

HIS Hachinski ischemic score, *ADAS* Alzheimer's Disease Assessment Scale, *y* years, *m* months

with ChEIs or other psychotropic drugs, and any patients who received medical treatment for AD were excluded from this study. Other exclusion criteria were a history of cerebral vascular disease diagnosis ("history of stroke" on the Hachinski ischemic scale), history of head trauma, seizures or other neurological disorders, mental retardation, alcohol and substance abuse, schizophrenia, major depressive disorder, bipolar disorder, and cardiac, pulmonary, vascular, metabolic, hematological conditions, or any other illnesses sufficiently severe to adversely affect cognition or functioning. This study was approved by the ethics committee of Teikyo University Chiba Medical Center (study number 11–17), and was performed in accordance with the Declaration of Helsinki. All patients and their closest caregivers gave written informed consent after a full explanation of all study procedures. Participants received SPECT and ADAS-cog at baseline and 18 months following treatment with the ChEIs donepezil or galantamine.

Assessment cognitive function and vascular risk factors

The ADAS-cog was used to assess AD and cognitive impairment severity (Rosen et al. 1984). The ADAS-cog is a rating instrument for assessing cognitive dysfunction in AD, consisting of 11 components for measuring cognitive function including word recall, word recognition, constructional praxis, orientation, naming, commands, ideational praxis, remembering test instructions, spoken language ability, word finding, and comprehension. Total ADAS-cog scores range from 0 to 70 and a higher total score indicates a poorer cognitive performance. ADAS-cog subscale were grouped into three domains, with one minor modification (Verma et al. 2015): language (spoken language, comprehension, word finding, naming, and remembering test instructions), memory (word recall, word recognition, and orientation) and praxis (commands, constructional praxis, and ideational praxis). Recovery was defined as an improvement of 3 points or more in the ADAS-cog total scores. Cognitive deficits severity was also assessed by the MMSE (Folstein et al. 1975), functional impairment severity was evaluated using the Functional Assessment Staging scale (FAST) (Reisberg et al. 1984), and the Hachinski ischemic scale (HIS) was used to evaluate the degree of vascular risk (Hachinski et al. 1975).

SPECT imaging

SPECT image scanning was performed using a dual-head rotating gamma camera (Millennium MG, GE healthcare, USA) with a parallel beam collimator, to permit a spatial resolution of 10 mm full width, at half maximum. Imaging began 20 min following intravenous injection of 222 MBq ^{123}I-IMP. We captured continuous images in 32 steps (64 projections), and each collected step counted for 30 s. Images were reconstructed by filtered backprojection, using attenuation corrected Butterworth and Ramp filters (Chang, 0.11/cm). Matrix size and slice thickness of SPECT images were 64 × 64 mm and 6.78 mm, respectively.

Image analysis

We evaluated the spatial distribution of abnormal rCBF by analyzing SPECT data using three dimensional stereotactic surface projection (3D-SSP), programed in Neurological Statistical Image Analyze Software (NEUROSTAT) (Minoshima et al. 1995). The original data were realigned to the bicommissural line (AC-PC line) and transferred into the stereotactic standard atlas following rotation and centering (Fig. 1), then maximum cortical activity was projected onto the brain surface pixels. All brain activity datasets were normalized to mean cortical activity. The pixel values corresponding to image data from each individual were compared to a database consisting of 18 normal subjects (age range from 60 to 81 years), followed by calculation of pixel-by-pixel z scores, which represents the degree of rCBF reduction. Pixel-by-pixel data were also used to divide the entire brain into segments at classified gyrus levels using the stereotactic extraction estimation method (SEE) level 3 (Mizumura et al. 2003; Hanyu et al. 2010; Kume et al. 2011).

Statistical analysis

Follow-up chnages in rCBF was calculated by subtracting the rCBF value at baseline from the value at 18 months for longitudinal analysis about hypoperfusion. Statistical analysis was performed using two-way repeated ANOVA. The relationships of 18 months ADAS-cog changes to changes in hypoperfusion were examined using the Pearson correlation coefficient. P value of less than 0.05 were considered significant, and the Bonferroni correction for multiple comparisons was used when appropriate (31 brain regions).

Results

Patient demographics at baseline and at 18 month follow-up

Neither ADAS-cog score or subscale (language, memory and praxis) scores changed significantly between baseline and follow up after 18 months of ChEIs treatments (Table 1). Seven out of 25 patients showed improvement (28%, Table 1).

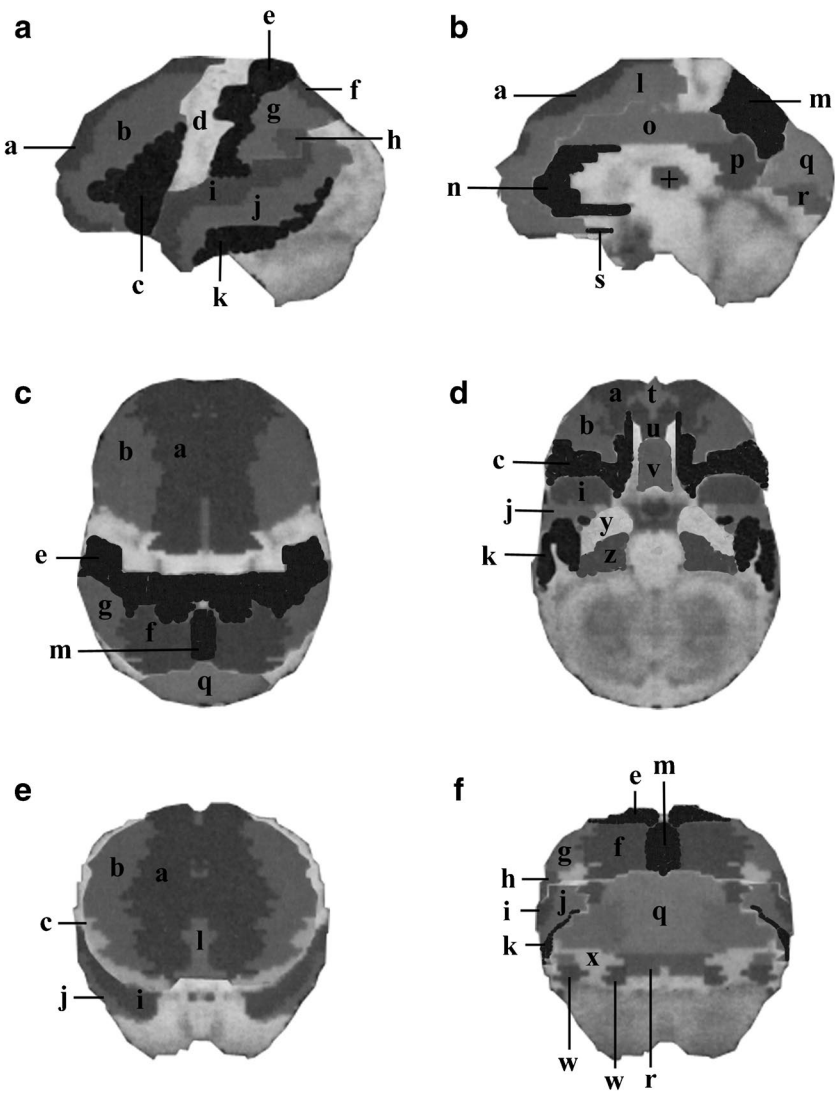

Fig. 1 Brain surface images. **a** lateral, **b** medial, **c** superior, **d** inferior, **e** anterior, **f** posterior. *a*, Superior frontal gyrus; *b*, Middle frontal gyrus; *c*, Inferior frontal gyrus; *d*, Precentral gyrus; *e*, Postcental gyrus; *f*, Superior parietal lobule; *g*, Inferior parietal lobule; *h*, Supramarginal gyrus; *i*, Superior temporal gyrus; *j*, Middle temporal gyrus; *k*, Inferior temporal gyrus; *l*, Medial frontal gyrus; *m*, Precuneus; *n*, Anterior cingulate; *o*, Cingulate gyrus; *p*, Posterior cingulate; *q*, Cuneus; *r*, Lingual gyrus; *s*, Subcallosal gyrus; *t*, Medial frontal gyrus; *u*, Orbital gyrus; *v*, Rectal gyrus; *w*, Fusiform gyrus; *x*, Inferior occipital gyrus; *y*, Uncus; *z*, Parahippocampal gyrus; +, Thalamus

Relationship between rCBF changes and time course following AD treatment and progression

Two patterns of rCBF, both deterioration in hypoperfusion and further reduction in hypoperfusion, showed a statistically significant difference after 18 months of ChEI treatment and AD progression. Deteriorated hypoperfusion was seen in the superior frontal gyrus of the frontal cortex, the superior parietal lobule, inferior parietal lobule, angular gyrus, postcentral gyrus and supramarginal gyrus of the parietal cortex, the transverse temporal gyrus of the temporal cortex, and the superior occipital and middle occipital gyri of the occipital cortex (Table 2, italics). In contrast, the inferior frontal gyrus, rectal gyrus, paracentral lobule and subcallosal gyrus of the frontal cortex, the thalamus, anterior cingulate and uncus of the limbic cortex all recovered hypoperfusion in spite of the progression of the disease, potentially due to ChEI treatment (Table 2, bold).

Correlation analysis of ADAS-cog score and rCBF changes from baseline to 18 month follow-up

We found a significant correlation between ADAS-cog changes and hypoperfusion, with significant changes from baseline to follow up at 18 months. There are two possible explanations for a positive relationship between changes in ADAS-cog scores and perfusion at baseline and at follow up: (1) both cognitive dysfunction and hypoperfusion worsened as the disease progressed, (2) hypoperfusion recovered and cognitive deficits improved (Fig. 2).

Deteriorated regions showing positive correlations with ADAS-cog total scores indicate that worsening hypoperfuison in these regions contributes to the deterioration of ADAS-cog score and include the superior parietal lobule, inferior parietal lobule, angular gyrus, and supramarginal gyrus of the parietal cortex (Table 3, italics). The superior parietal lobule, inferior parietal lobule and supramarginal

Table 2 Brain regions showing significant changes in hypoperfusions after 18 months treatments

		1st	2nd	Time	Lateral
< Frontal cortex >					
Superior frontal gyrus	L	1.048 ± 0.376	1.168 ± 0.503	0.025*	0.376
	R	1.119 ± 0.509	1.328 ± 0.655		
Middle frontal gyrus	L	1.301 ± 0.677	1.258 ± 0.596	0.473	0.370
	R	1.353 ± 0.570	1.509 ± 0.756		
Inferior frontal gyrus	L	1.745 ± 1.059	1.547 ± 0.783	0.038*	0.554
	R	1.631 ± 0.886	1.390 ± 0.779		
Medial frontal gyrus	L	1.434 ± 0.402	1.443 ± 0.728	0.727	0.797
	R	1.413 ± 0.496	1.443 ± 0.728		
Orbital gyrus	L	2.253 ± 1.320	2.147 ± 1.347	0.047*	0.609
	R	2.653 ± 1.121	2.074 ± 1.284		
Rectal gyrus	L	2.288 ± 0.920	1.770 ± 1.126	< 0.001***	0.786
	R	2.232 ± 1.121	1.682 ± 1.020		
Paracentral lobule	L	0.586 ± 0.408	0.460 ± 0.388	0.036*	0.858
	R	0.576 ± 0.426	0.509 ± 0.416		
Precentral gyrus	L	0.694 ± 0.557	0.627 ± 0.384	0.754	0.320
	R	0.742 ± 0.525	0.854 ± 0.664		
Subcallosal gyrus	L	1.950 ± 1.339	1.443 ± 1.329	0.002**	0.823
	R	1.818 ± 1.172	1.431 ± 1.069		
<Parietal cortex >					
Superior parietal lobule	L	0.555 ± 0.455	0.958 ± 0.562	< 0.001***	0.003**
	R	1.168 ± 0.740	1.357 ± 0.797		
Inferior parietal lobule	L	0.609 ± 0.597	1.100 ± 0.708	< 0.001***	0.022*
	R	1.189 ± 0.823	1.668 ± 1.397		
Angular gyrus	L	0.663 ± 0.614	1.316 ± 0.918	< 0.001***	0.056 [a]
	R	1.290 ± 1.107	1.846 ± 1.711		
Postcentral gyrus	L	0.445 ± 0.372	0.601 ± 0.516	0.018*	0.018*
	R	0.757 ± 0.475	0.941 ± 0.707		
Precuneus	L	0.676 ± 0.486	0.715 ± 0.487	0.275	0.327
	R	0.750 ± 0.502	0.878 ± 0.526		
Supramarginal gyrus	L	0.395 ± 0.474	0.940 ± 0.834	< 0.001***	0.023*
	R	0.878 ± 0.815	1.565 ± 1.441		
< Temporal cortex>					
Superior temporal gyrus	L	1.490 ± 0.492	1.328 ± 0.524	0.846	0.906
	R	1.385 ± 0.578	1.400 ± 0.692		
Middle temporal gyrus	L	1.106 ± 0.414	1.090 ± 0.519	0.243	0.050 [a]
	R	1.381 ± 0.742	1.598 ± 1.132		
Inferior temporal gyrus	L	1.248 ± 0.661	1.209 ± 0.633	0.820	0.015*
	R	1.795 ± 0.915	1.877 ± 1.298		
Transverse temporal gyrus	L	0.128 ± 0.328	0.462 ± 0.931	0.010*	0.127
	R	0.445 ± 0.602	0.754 ± 1.153		
< Occipital cortex >					
Superior occipital gyrus	L	0.331 ± 0.357	0.914 ± 0.883	0.002**	0.203
	R	0.916 ± 1.306	1,018 ± 1.240		
Middle occiptal gyrus	L	0.574 ± 0.402	0.778 ± 0.722	0.020*	0.577
	R	0.714 ± 0.775	0.854 ± 0.915		
Inferior occipital gyrus	L	0.436 ± 0.714	0.389 ± 0.464	0.948	0.908
	R	0.412 ± 0.572	0.448 ± 0.622		
Cuneus	L	0.414 ± 0.378	0.581 ± 0.456	0.156	0.066
	R	0.697 ± 0.469	0.720 ± 0.526		

Table 2 (continued)

		1st	2nd	Time	Lateral
Fusiform gyrus	L	1.202 ± 0.598	1.116 ± 0.605	0.189	0.019*
	R	1.785 ± 0.979	1.600 ± 1.126		
Lingual gyrus	L	0.425 ± 0.680	0.350 ± 0.472	0.661	0.335
	R	0.587 ± 0.906	0.588 ± 0.981		
< Limbic cortex >					
Thalamus	L	1.342 ± 0.895	1.009 ± 0.726	0.004**	0.012*
	R	0.807 ± 0.506	0.650 ± 0.465		
Cingulate gyrus	L	1.218 ± 0.550	1.160 ± 0.404	0.429	0.774
	R	1.251 ± 0.569	1.202 ± 0.506		
Parahippocampal gyrus	L	1.102 ± 0.904	1.041 ± 0.815	0.191	0.588
	R	1.270 ± 0.743	1.106 ± 0.787		
Anterior cingulate	L	1.640 ± 0.570	1.414 ± 0.565	< 0.001***	0.901
	R	1.632 ± 0.632	1.383 ± 0.595		
Posterior cingulate	L	0.762 ± 0.443	0.811 ± 0.437	0.671	0.326
	R	0.904 ± 0.427	0.891 ± 0.428		
Uncus	L	1.740 ± 0.784	1.549 ± 0.985	0.015*	0.114
	R	1.440 ± 0.840	1.148 ± 0.738		

Brain regions in *italic* was deterioration of hypoperfusion whereas regions in **bold** was recovery of hypoperfusion, compared to the baseline

*p < 0.05, **p < 0.01, ***p < 0.001

ADAS Alzheimer's Disease Assessment Scale

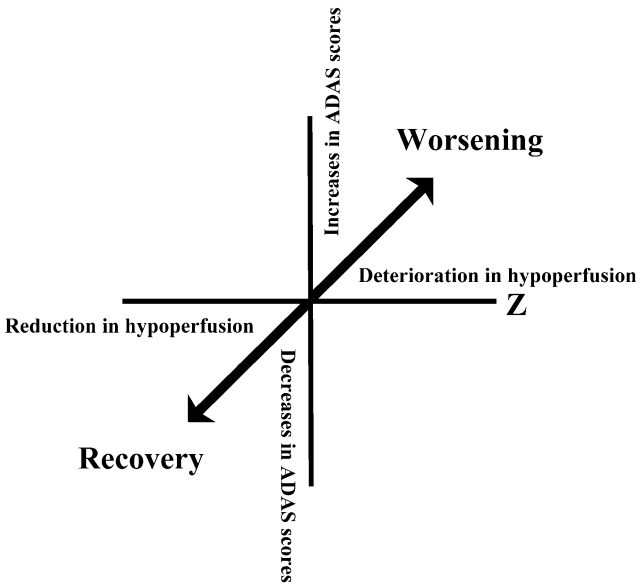

Fig. 2 Positive correlation between ADAS scores and hypoperfusion indicates either "worsening" or "recovery". Z scores showed a decrease in rCBF for all AD patients. Z scores were calculated by 3D-SSP, a higher z score represents a more severe reduction of rCBF. Increases in ADAS scores indicates "worsening" AD

gyrus of the parietal cortex were significantly related to the ADAS-cog language subscale (Table 3), and the angular gyrus of the parietal cortex showed a significant relationship with the ADAS-cog memory subscale (Table 3).

On the other hands, the paracentaral lobule of the frontal cortex (Table 3, in bold) showed a positive correlation with total ADAS-cog score, indicating that recovered hypoperfusion in these regions contributed to recovery of ADAS-cog scores, potentially due to ChEI treatment. Additionally, both the rectal gyrus of the frontal cortex and the anterior cingulate of the limbic cortex showed significant relationships with the ADAS-cog praxis subscale (Table 3).

Some regions without changes in hypoperfusion, such as the precuneus of the parietal cortex, showed a significant relationship with total ADAS-cog and the memory subscale (Table 3). We also found relahionships between the precentral gyrus of the frontal cortex and the ADAS-cog memory subscale, as well as between the superior temporal gyrus of the temporal cortex and the ADAS-cog praxis subscale (Table 3).

Discussion

Hypoperfusion changes from baseline to follow up at 18 months

Twenty-eight percent of patients showed recovery after 18 months ChEI treatment, while 24% of patients with late-onset patients showed worsening AD (Table 1). This is comparable to a previous data showing 25–50% recovery after 6 months of ChEI treatment (Giacobini 2000).

Table 3 Relationships between changes in ADAS-cog and rCBF during 18 months follow-ups

		ADAS-cog Total	ADAS-cog Language	ADAS-cog Memory	ADAS-cog Praxis
< Frontal cortex >					
Superior frontal gyrus	L	0.162	−0.001	0.182	0.172
	R	−0.123	−0.219	−0.180	−0.079
Middle frontal gyrus	L	0.068	0.052	0.061	0.044
	R	−0.034	0.041	−0.140	−0.084
Inferior frontal gyrus	L	−0.109	−0.039	−0.227	0.070
	R	−0.060	−0.085	−0.175	0.138
Medial frontal gyrus	L	−0.002	−0.166	−0.191	0.300
	R	0.064	0.117	−0.179	0.343
Orbital gyrus	L	−0.008	−0.039	−0.099	0.209
	R	−0.036	−0.024	−0.077	0.197
Rectal gyrus	L	0.055	0.009	−0.347	0.472*
	R	−0.059	0.096	−0.327	0.369
Paracentral lobule	L	0.313	0.303	0.255	0.157
	R	0.407*	0.207	0.270	0.075
Precentral gyrus	L	0.193	−0.145	0.419*	0.211
	R	−0.061	−0.062	0.002	−0.176
Subcallosal gyrus	L	0.111	0.049	−0.088	0.209
	R	−0.030	−0.20	−0.191	0.248
<Parietal cortex >					
Superior parietal lobule	L	0.304	0.229	0.360	0.082
	R	0.506**	0.398*	0.324	0.249
Inferior parietal lobule	L	0.321	0.325	0.185	0.220
	R	0.501*	0.521**	0.303	0.167
Angular gyrus	L	0.349	0.310	0.273	0.270
	R	0.459*	0.332	0.399*	0.228
Postcentral gyrus	L	−0.136	0.061	−0.138	−0.329
	R	−0.141	0.117	−0.173	−0.331
Precuneus	L	0.427*	0.142	0.538**	0.235
	R	0.139	−0.120	0.261	0.089
Supramarginal gyrus	L	0.423*	0.416*	0.298	0.361
	R	0.349	0.305	0.212	0.254
< Temporal cortex>					
Superior temporal gyrus	L	−0.073	−0.096	0.079	−0.150
	R	−0.251	−0.219	−0.226	−0.433*
Middle temporal gyrus	L	0.150	0.340	−0.134	−0.018
	R	−0.207	−0.185	−0.184	−0.238
Inferior temporal gyrus	L	0.081	0.058	0.146	0.088
	R	−0.212	−0.236	−0.188	−0.048
Transverse temporal gyrus	L	−0.029	−0.021	0.117	−0.269
	R	−0.001	0.044	−0.013	−0.177
< Occipital cortex >					
Superior occipital gyrus	L	0.073	0.109	−0.023	0.077
	R	0.111	0.142	0.081	0.355
Middle occiptal gyrus	L	0.076	0.086	0.076	0.034
	R	−0.279	−0.341	−0.332	−0.117
Inferior occipital gyrus	L	0.196	0.038	0.189	0.259
	R	−0.041	−0.122	−0.050	−0.078
Cuneus	L	−0.094	−0.149	0.018	−0.040
	R	0.043	0.149	−0.121	0.045

Table 3 (continued)

		ADAS-cog Total	ADAS-cog Language	ADAS-cog Memory	ADAS-cog Praxis
Fusiform gyrus	L	−0.210	−0.053	−0.235	0.033
	R	−0.240	−0.245	−0.169	−0.080
Lingual gyrus	L	−0.058	−0.148	−0.013	0.207
	R	0.149	−0.042	0.068	−0.277
< Limbic cortex >					
Thalamus	L	0.065	−0.078	0.123	0.104
	R	0.033	0.018	0.037	−0.217
Cingulate gyrus	L	0.269	0.125	0.163	0.034
	R	0.339	0.316	0.118	0.037
Parahippocampal gyrus	L	0.275	0.073	0.230	0.274
	R	−0.043	−0.147	−0.059	−0.130
Anterior cingulate	L	0.233	0.160	−0.173	0.536**
	R	0.176	0.156	−0.147	0.418*
Posterior cingulate	L	0.332	0.520**	0.148	0.068
	R	0.021	0.077	−0.048	0.085
Uncus	L	0.085	0.124	0.157	0.085
	R	−0.387	−0.658***	−0.233	−0.436*

ADAS Alzheimer's Disease Assessment Scale

*p < 0.05, **p < 0.01, ***p < 0.001

Here we observed both worsening of rCBF reduction in some regions and recovery in others at the 18 month follow up of late-onset AD patients. We saw significant increases in rCBF reduction z scores in 5 regions of the parietal cortex, 2 regions of the occipital cortex, 1 region of the frontal cortex, and 1 region of the temporal cortex, while significant decreases in rCBF reduction z scores were seen in 4 regions of the frontal cortex and 3 regions of the limbic cortex.

The present study is focused on late-onset AD, and shows that rCBF decreased in the parietal cortex but increased in the frontal and limbic cortices after 18 months of follow-up under ChEI treatment (Table 2). We previously showed that baseline hypoperfusion was prominent in the frontal, temporal and limbic cortices in late-onset AD, with a lesser reduction in the parietal cortex (Takahashi et al. 2017), suggesting that baseline hypoperfusion could occur specifically in late-onset AD. In contrast, previous studies have shown hypoperfuison in the parietal and temporal cortices in the early stages of early-onset AD, while reduced perfusion in the frontal cortex is seen in advanced stages (Kumar et al. 1991; Waldemar et al. 1994). SPECT imaging indicates that late-onset AD showa a pattern of hypoperfusion distinct from early-onset AD at baseline and during progression. Therefore, SPECT could be utilized as routine test for late-onset AD in the clinic.

Previous SPECT studies have also shown rCBF increases, primarily in the frontal lobe, in response to ChEI treatment (Nakano et al. 2001; Nobili et al. 2002; Ushijima et al. 2006). PET studies have demonstrated that treatment with the ChEI rivastigmine increased glucose metabolism in the frontal cortex (Potkin et al. 2001; Stefanova et al. 2006), and 1 year of ChEI treatment increased rCBF on SPECT mainly in the frontal cortex including anterior cingulate in cases of late-onset AD (Tateno et al. 2008; Chaudhart et al. 2013; Shimizu et al. 2015). Therefore, ChEI treatment increases rCBF in the frontal cortex in both early and late-onset AD. However, other regions including the posterior cingulate or precuneus also showed an increase in rCBF following ChEI treatment (Tateno et al. 2008; Chaudhart et al. 2013; Shimizu et al. 2015). Additional study is needed to address this problem.

Frontal cortex

Siginificant recovery of hypoperfusion was seen in the inferior frontal gyrus, orbital gyrus, rectal gyrus, paracentral lobule and subcallosal gyrus of the frontal cortex (Table 2, bold), whereas increased hypoperfusion was seen in the superior frontal gyrus (Table 2, italics) at follow up. In spite of recovery observed in 5 regions, some significant relationships between rCBF changes and ADAS-cog score may reflect small relationships between ChEI treatment and rCBF. Factors other than rCBF could also be involved in the effects of ChEI treatment.

The rectal gyrus showed recovery of hypoperfusion after 18 months ChEI treatment ($p < 0.001$, Table 2), and rectal hypoperfusion changes remained significant after Bonferroni correction for multiple comparisons ($p < 0.05/31 = 0.0016$).

We also found a positive correlation between changes in hypoperfusion over 18 months and ADAS-cog subscale praxis scores in the rectal gyrus (Table 3). Since the rectal gyrus showed prominent hypoperfusion, it could be a useful clinical landmark in late-onset AD patients.

Hypoperfusions in the inferior frontal, orbital, and subcallosal gyri were reduced at folow up following ChEI treatment (Table 2), indicating that ChEI seemed to work in thses regions. However, hypoperfusion changes in these regions were unrelated to ADAS-cog score changes (Table 3). Hypoperfusion in the inferior frontal gyrus, but not in the orbital or subcallosal gyrus, showed significant correlations with total ADAS-cog scores at baseline, although prominent hypoperfusion was also observed (Takahashi et al. 2017). Another SPECT study showed that AD patients with depression showed inferior frontal region hypoperfusion (Honda et al. 2014). Lower pretreatment rCBF levels in the orbitofrontal cortex also predicted more improvement in ADAS-cog score following 6 months of donepezil therapy in AD patients (Hongo et al. 2008). From a clinical perspective, it is likely that these regions are involved in late-onset AD pathology.

A small but significant recovery in hypoperfusion were seen in the paracentral lobule (Table 2), and was significantly related to changes in total ADAS-cog scores (Table 3). Hypoperfusion in the paracentral lobule at baseline also had a small but significant relationship to ADAS-cog memory subscale (Takahashi et al. 2017). This region may be vulnerable to the progression of late-onset AD as well as ChEI treatment. Future studies are needed to understand the role of this region in late stage AD.

The superior frontal gyrus showed increased hypoperfusion, indicating disease progression as reflected by ADAS-cog scores (Table 2). A recent PET study of depressive AD patients showed rCBF decreases in the superior frontal gyrus (Lee et al. 2006). Another PET study showed negative correlations between episodic memory deficits and the superior frontal gyrus in AD patients (Desgranges et al. 2002). However, we did not see significant relationships between changes in hypoperfusion and ADAS-cog score after 18 months (Table 3), or between hypoperfuion and baseline ADAS-cog scale (Takahashi et al. 2017). Additional study of the role of the superior frontal gyrus is needed.

Parietal cortex

The superior parietal lobule, inferior parietal lobule, angular gyrus, postcentral gyrus and supramarginal gyrus of the parietal cortex (Table 2, italics) showed significant changes in hypoperfusion between baseline and follow-up. All regions except the postcentral gyrus remained significant after Bonferroni correction for multiple comparisons ($p < 0.05/\ 31 = 0.0016$). This is consistent with another recent study showing rCBF reductions in the superior parietal lobule, inferior parietal lobule, angular gyrus and supramarginal gyrus of the parietal cortex in rapidly progressing late-onset AD patients (Hanyu et al. 2010).

The superior parietal lobule, inferior parietal lobule, angular gyrus, postcentral gyrus and supramarginal gyrus, but not the postcentral gyrus, were related to total ADAS-cog scores (Table 3). The superior parietal lobule, inferior parietal lobule, and supramarginal gyrus showed significant relationships with the ADAS-cog language subscale, while the angular gyrus had a significant relationship to the ADAS-cog memory subscale (Table 3). At baseline, hypoperfusion in the inferior parietal lobule, angular gyrus, and supramarginal gyrus of the parietal cortex were significantly related to total ADAS-cog and subscale scores (Takahashi et al. 2017), indicating that these regions could be involved in the clinical process of late onset AD. Interestingly, lesions in the inferior parietal lobule, and angular and supramarginal gyri of the parietal cortex produce lexical and phonological agraphia (Roeltgen and Heilman 1984), suggesting that these sites might play a role in retrieval during writing in late-onset AD.

Hypoperfusion chnages in the precuneus was significantly related to total ADAS-cog and memory subscale changes between baseline and follow up (Table 3), although hypoperfusion did not show a significant change at 18 months (Table 2). We note that longitudinal studies showed a reduction in brain hypoperfusion in the precuneus of the parietal cortex in mild cognitive impairment patients who converted to AD (Hirano et al. 2005) as well as mild AD patients (Kogure et al. 2000). Additionally, a PET study showed a significant correlation between episodic memory scores and activation of the precuneus (Fletcher et al. 1995). Future studies are needed to understand the clinical role of this region in memory processes.

In early and late-onset AD, hypoperfusion changes in the parietal region were significantly correlated with the progression of cognitive dysfunction (Kemp et al. 2003; Nagahama et al. 2003; Hanyu et al. 2010; Kimura et al. 2012), and overlap with the present results. The parietal cortex may be the core region involved in the progression of cognitive deficits and this issue should be addressed in future studies.

Occipital cortex

Significantly incerasesd hypoperfusion was seen in the superior occipital gyrus and middle occipital gyrus at 18 month follow up (Table 2), but that hypoperfusion were unrelated to total and subscale ADAS-cog scores (Table 3).

Limbic cortex

The thalamus, antierior cingulate, and uncus of the limbic cortex (Table 2, bold) showed recovery of hypoperfusion, but these changes did not show any relationship to changes in total ADAS-cog scores (Table 3).

The anterior cingulate showed hypoperfusion recovery at 18 months of ChEI treatment (Table 2), which remained significant after Bonferroni correction for multiple comparisons ($p < 0.05/31 = 0.0016$). We also found a positive relationship between hypoperfusion changes in the anterior cingulate and ADAS-cog praxis subscale (Table 3). Hypoperfusion in the anterior cingulate was related to baseline performance on language subscales in late-onset AD (Takahashi et al. 2017). The anterior cingulate plays a part in language subscale performance at early stages and praxis subscale performance at advanced stages of late-onset Alzheimer's disease. Previous SPECT studies also showed that chronic ChEI treatments for 4 to 12 months increase rCBF in the anterior cingulate of the limbic cortex in AD patients (Nakano et al. 2001; Ceravolo et al. 2004). It is likely that the anterior cingulate is a site of ChEI action. A recent study also demonstrated that the anterior cingulate engages motivational incentives (Rushworth et al. 2007; Kouneiher et al. 2009). Motivation could be involved in the praxis deficits observed in late-onset AD. It could also be that ChEIs recover praxis deficits by restoring hypoperfusion in the anterior cingulate in late-onset AD patients.

Thalamic hypoperfusion was reduced (Table 2), potentially due to ChEI treatment. However, we did not see any relationship between hypoperfusion changes and changes in ADAS-cog scores (Table 3). Our recent study also failed to see a significant relationship between pretreatment hypoperfusion and total or subscale ADAS-cog scores (Takahashi et al. 2017). Future studies are needed to understand the role of the thalamus in late-onset AD.

Hypoperfusion changes in the posterior cingulate showed a significant relationship with changes in ADAS-cog language subscale between baseline and follow up (Table 3). However, hypoperfusion in the posterior cingulate gyrus did not change significantly (Table 2). Hypoperfusion in the posterior cingulate showed significant correlations with total ADAS-cog and as well as language and memory subscalae scores at baseline (Takahashi et al. 2017). In a previous longitudinal study, brain hypoperfusion was reduced in the posterior cingulate gyrus in mild cognitive impairment subjects who converted to AD (Hirano et al. 2005). Additional sutdy is needed to address the role of the posterior cingulate in the pathology of late-onset AD.

The uncus showed recovery of hypoperfusion at 18 month follow up (Table 2). These change in hypoperfusion were negatively related to changes in ADAS-cog language and memory subscales between baseline and follow up (Table 3). However, the meaning of a negative relationship is unknown. We speculate that it could be a compensatory phenomenon.

Conclusion

After 18 months of ChEI treatment, some regions were further hypoperfused, reflecting disease worsening while other regions showed alleviated hypoperfusion, potentially because of ChEI treatment. Prominent rCBF decreases were in the superior parietal lobule, inferior parietal lobule, angular gyrus, and supramarginal gyrus of the parietal cortex, and the superior occipital of the occipital cortex. Prominent rCBF increases were in the rectal and subcallosal gyri of the frontal cortex, and the thalamus and anterior cingulate of the limbic cortex. These regions showed significant relationships with total ADAS-cog and language, memory and praxis subscales scores.

Funding This research did not receive any specific grant from any funding agencies in the public, commercial or not-for-profit sectors.

Compliance with Ethical Standards

Conflict of interest Dr. Shirayama has received research support from Eli Lilly, Eisai, MSD, Pfizer, Takeda and Mitsubishi-Tanabe. Dr. Iyo has received consultant fees from Eli Lilly, Sumitomo, Dainippon, Pfizer and Abbott.
Drs. Takahashi, Oda, Yoshino and Sato have no competing interests.

Ethical approval All procedures performed in this study were in accordance with the ehical standards of the institutional research committee and with 1964 Helsinki Declaration and its later amendments or comparable ethical standards. This study was approved by the ehics committee of Teikyo University Chiba Medical Center.

Informed consent Informed consent was obtained from all individual participants included in this study.

References

American Psychiatric Association (1994). *Diagnostic and statistic manual of mental disorders (DSN-IV-TR)*, 4th edn., text rev). Washington DC: American Psychiatric Press.

Canu, E., Frisoni, G. B., Agosta, F., Pievani, M., Bonetti, M., & Filippi, M. (2012). Early and late onset Alzheimer's disease patients have distinct patterns of white matter damage. *Neurobiology of Aging, 33*, 1023–1033.

Cavedo, E., Pievani, M., Boccardi, M., Galluzzi, S., Bocchetta, M., Bonetti, M., et al. (2014). Medial temporal atrophy in early and late-onset Alzheimer's disease. *Neurobiology of Aging, 35*, 2004–2012.

Ceravolo, R., Volterrani, D., Toqnoni, G., Dell'Aqnello, G., Manca, G., Kiferie, L., et al. (2004). Cerebral perfusional effects of cholinesterase inhibitors in Alzheimer disease. *Clinical Neuropharmacology, 27*, 166–170.

Chaudhart, S., Scouten, A., Schwindt, G., Janik, R., Lee, W., Sled, J. G., et al. (2013). Hemodynamic effects of cholinesterase inhibition

in mild Alzheimer's disease. *Journal of Magnetic Resonance Imaging, 28*, 26–35.

Desgranges, B., Baron, J. C., Giffard, B., Chételat, G., Lalevée, C., de la Sayette, V., et al. (2002). The neural basis of instruction in free recall and cued recall: a PET study in Alzheimer's disease. *Neuroimage, 17*, 1658–1664.

Dubois, B., Feldman, H. H., Jacova, C., Cummings, J. L., DeKosky, S. T., Barberger-Gateau, P., et al. (2010). Revising the definition of Alzheimer's disease: a new lexicon. *Lancet Neurology, 9*, 1118–1127.

Fletcher, P. C., Frith, C. D., Grasby, P. M., Shallice, T., Frackowiak, R. S., & Dolan, R. J. (1995). Brain systems for encoding and retrieval of auditory-verbal memory. An in vivo study in humans. *Brain, 118*, 401–416.

Folstein, M. F., Folstein, S. E., & McHugh, P. R. (1975). Mini-mental state. A practical method for grading the cognitive state of patients for the clinicians. *Journal of Psychiatric Research, 12*, 189–198.

Frisoni, G. B., Pievani, M., Testa, C., Sabattoli, F., Bresciani, L., Bonetti, M., et al. (2007). The topography of grey matter involvement in early and late onset Alzheimer's disease. *Brain, 130*, 720–730.

Giacobini, E. (2000). Cholinestrase inhibitor therapy stabilize symptoms of Alzheimer disease. *Alzheimer Disease and Associated Disorders, 14 suppl 1*, S2-S10.

Grady, C. L., Haxby, J. V., Horwitz, B., Berg, G., & Rapoport, S. I. (1987). Neuropsychological and cerebral metabolic function in early vs late onset dementia of the Alzheimer type. *Neuropsychologia, 25*, 807–816.

Hachinski, V. C., Iliff, L. D., Zilhka, E., Du Boulay, G. H., McAllister, V. L., Marshall, J., et al. (1975). Cerebral blood flow in dementia. *Archives of Neurology, 32*, 632–637.

Hanyu, H., Sato, T., Hirao, K., Kanetaka, H., Iwamoto, T., & Koizumi, K. (2010). The progression of cognitive deterioration and regional cerebral blood flow patterns in Alzheimer's disease: a longitudinal SPECT study. *Journal of Neurological Sciences, 290*, 96–101.

Hirano, K., Ohnishi, T., Hirata, Y., Yamashita, F., Mori, T., Moriguchi, Y., et al. (2005). The prediction of rapid conversion of Alzheimer's disease in mild cognitive impairment using regional cerebral blood flow SPECT. *Neuroimage, 28*, 1014–1021.

Honda, H., Terada, S., Sato, S., Oshima, E., Ikeda, C., Nagao, S., et al. (2014). Subjective depressive mood and regional blood flow in mild Alzheimer's disease. *International Psychogeriatrics, 26*, 817–823.

Hongo, J., Nakaaki, S., Shinagawa, Y., Murata, Y., Sato, J., Tatsumi, H., et al. (2008). SPECT-identified neuroanatomical predictor of the cognitive effects of donepezil treatment in patients with Alzheimer's disease. *Dementia and Geriatric Cognitive Disorders, 26*, 556–566.

Ishii, K., Kawachi, T., Sasaki, H., Kono, A. K., Fukuda, T., Kojima, Y.,et al (2005). Voxel-based morphometric comparison between early- and late-onset mild Alzheimer's disease and assessment of diagnostic performance of Z score images. *American Journal of Neuroradiology, 26*, 333–340.

Johnson, K. A., Jones, K., Holman, B. L., Spiers, P. A., Satllin, A., & Albert, M. S. (1998). Preclinical prediction of Altzheimer's disease using SPECT. *Neurology, 50*, 1563–1571.

Joubert, S., Gour, N., Guedi, E., Didic, M., Guériot, C., Koric, L., et al. (2016). Early-onset and late-onset Alzheimer's disease are associated with distinct patterns of memory impaiment. *Cortex, 74*, 217–232.

Kaiser, N. C., Melrose, R. J., Liu, C., Sultzer, D. L., Jimenez, E., Su, M., et al. (2012). Neuropsychological and neuroimaging markers in early versus late-onset Alzheimer's disease. *American Journal of Alzheimer's Disease and Other Dementias, 27*, 520–529.

Keller, C., Kadir, A., Forsberg, A., Porras, O., & Noerberg, A. (2011). Long-term effects of galantamine treatment on brain functional activities as measured by PET in Alzheimer's disease patients. *Journal of Alzheimer's Disease, 24*, 109–123.

Kemp, P. M., Holmes, C., Hoffmann, S. M., Bolt, L., Holmes, R., Rowden, J., et al. (2003). Alzheimer's disease: differences in technetium-99m HMPAO SPECT scan findings between early onset and late onset dementia. *Journal of Neurology, Neurosurgery, and Psychiatry, 74*, 715–719.

Kimura, N., Kumamoto, T., Masuda, T., Hanaoka, T., Okazaki, T., & Arakawa, R. (2012). Evaluation of the cerebral blood flow changes during long-term donepezil therapy in patients with Alzheimer's disease using 3DSRT. *Journal of Neuroimaging, 22*, 299–304.

Kogure, D., Matsuda, H., Ohnishi, T., Asada, T., Uno, M., Kunihiro, T., et al. (2000). Longitudinal evaluation of early Alzheimer's disease using brain perfusion SPECT. *Journal of Nuclear Medicine, 41*, 1155–1162.

Kouneiher, F., Charron, S., & Koechlin, E. (2009). Motivation and cognitive control in the human prefrontal cortex. *Nature Neuroscience, 12*, 939–945.

Kumar, A., Schapiro, M. B., Grady, C., Haxby, J. V., Wagner, E., Salerno, J. A., et al. (1991). High-resolution PET studies in Alzheimer's disease. *Neuropsychopharmacology, 4*, 35–46.

Kume, K., Hanyu, H., Sato, T., Hirao, K., Shimizu, S., Kanetaka, H., et al. (2011). Vascular risk factors are associated with faster decline of Alzheimer disease: a longitudinal SPECT study. *Journal of Neurology, 258*, 1295–1303.

Lee, D. Y., Choo, I. H., Jhoo, J. H., Kim, K. W., Youn, J. C., Lee, D. S., et al. (2006). Frontal dysfunction underlie depressive syndrome in Alzheimer disease: a FDG-PET study. *American Journal of Geriatric Psychiatry, 14*, 625–628.

Li, W., Antuono, P. G., Xie, C., Chen, G., Jones, J. L., Ward, B. D., et al. (2012). Changes in regional cerebral blood flow and functional connectivity in the cholinergic pathway associated with cognitive performance in subjects with mild Alzheimer's disease after 12-week donepezil treatment. *Neuroimage, 60*, 1083–1091.

McKhann, G., Drachman, D., Folstein, M., Katzman, R., Price, D., & Stadlan, E. M. (1984). Clinical diagnosis of Alzheimer's disease: report of the NINCDS-ADRDA work group under the auspices of Department of Health and Human Services Task Force on Alzheimer's disease. *Neurology, 34*, 939–944.

Minoshima, S., Frey, K. A., Koeppe, R. A., Foster, N. L., & Kuhl, D. E. (1995). A diagnostic approach in Alzheimer's disease using three-dimensional stereotactic surface projections of fluorine-18-FDG PET. *Journal of Nuclear Medicine, 36*, 1238–1248.

Mizumura, S., Kumita, S., Cho, K., Ishihara, M., Nakajo, H., Toba, M., et al. (2003). Development of quantitative analysis method for stereotactic brain image: assessment of reduced accumulation in extent and severity using anatomical segmentation. *Annals of Nuclear Medicine, 17*, 289–295.

Möller, C., Vrenken, H., Jiskoot, L., Versteeg, A., Barkhof, F., Scheltens, P., et al. (2013). Different patterns of gray matter atrophy in early-and late-onset Alzheimer's disease. *Neurobiology of Aging, 34*, 2014–2022.

Nagahama, Y., Nabatame, H., Okina, T., Yamauchi, H., Narita, M., Fujimoto, N., et al. (2003). Cerebral correlations of the cognitive decline in probable Alzheimer's disease. *European Neurology, 50*, 1–9.

Nakano, S., Asada, T., Matsuda, H., Uno, M., & Takasaki, M. (2001). Donepezil hydrochloride preserves regional cerebral blood flow in patients with Alzheimer's disease. *Journal of Nuclear Medicine, 41*, 1441–1445.

Nobili, F., Vitali, P., Canfora, M., Girtler, N., De Leo, C., Mariani, G., et al. (2002). Effects of long-term Donepezil therapy on rCBF of Alzheimer's patients. *Clinical Neurophysiology, 113*, 1241–1248.

Potkin, S. G., Anand, R., Fleming, K., Alva, G., Keator, D., Carreon, D., et al. (2001). Brain metabolic and clinical effects of

rivastigmine in Alzheimer's disease. *International Journal of Neuropsychopharmacology, 4*, 223–230.

Reisberg, B., Ferris, S. H., Anand, R., de Leon, M. J., Schneck, M. K., Buttinger, C., et al. (1984). Functional staging of dementia of the Alzheimer's type. *Annals of the New York Academy of Sciences, 435*, 481–483.

Roeltgen, D. P., & Heilman, K. M. (1984). Lexical agraphia. Further support for the two-system hypothesis of linguistic agraphia. *Brain, 107*, 811–827.

Rosen, W. G., Mohs, R. C., & Davis, K. L. (1984). A new rating scale for Alzheimer's disease. *American Journal of Psychiatry, 141*, 1356–1364.

Rushworth, M. F., Buckley, M. J., Behrens, T. E., Walton, M. E., & Bennerman, D. M. (2007). Functional organization of the medial frontal cortex. *Current Opinion of Neurobiology, 17*, 220–227.

Sá, F., Pinto, P., Cunha, C., Lemos, R., Letra, L., Simões, M., et al. (2012). Differences between early and late-onset Alzheimer's disease in neuropsychological tests. *Frontiers in Neurology, 14*, 81.

Shimizu, S., Kanetake, H., Hirose, D., Sakurai, H., & Hanyu, H. (2015). Differential effects of acetylcholinesterase inhibitors on clinical responses and cerebral blod flow changes in patients with Alzheimer's disease: a 12-month, randomized, and open-label trial. *Dementia and Geriatric Cognitive Disorders Extra, 5*, 135–146.

Stefanova, E., Wall, A., Almkvist, O., Nilsson, A., Forsberg, A., Långström, B., et al. (2006). Longitudinal PET evaluation of cerebral glucose metabolism in rivastigmine treated patients with mild Alzheimer's disease. *Journal of Neural Transmission, 113*, 205–218.

Takahashi, M., Oda, Y., Okubo, T., & Shirayama, Y. (2017). Relationships between cognitive impairment on ADAS-cog and regional cerebral blood flow using SPECT in late-onset Alzheimer's disease. *Journal of Neural Transmission, 124*, 1109–1121.

Tateno, M., Kobayashi, S., Utsumi, K., Morii, H., & Fujii, K. (2008). Quantitative analysis of the effects of donepezil on regional cerebral blood flow in Alzheimer's disease by using an automated program, 3DSRT. *Neuroradiology, 50*, 723–727.

Ushijima, Y., Okuyama, C., Mori, S., Kubota, T., Nakai, T., & Nishimura, T. (2006). Regional cerebral blood flow in Alzheimer's disease: comparison between short and long-term donepezil therapy. *Annals of Nuclear Medicine, 20*, 425–429.

Verma, N., Beretvas, S. N., Pascual, B., Masdeu, J. C., & Markey, M. K. (2015). New scoring methodology improves the sensitivity of the Alzheimer's Disease Assessment Scale-Cognitive subscale (ADAS-Cog) in clinical trials. *Alzheimers Research & Therapy, 7*, 64.

Waldemar, G., Bruhn, P., Kristensen, M., Johnson, A., Paulson, O. B., & Lassen, N. A. (1994). Heterogeneity of neocortical cerebral blood flow deficits in dementia of the Alzheimer type: a [^{99}Tc]-d,l-HMPAO SPECT study. *Journal of Neurology, Neurosurgery, and Psychiatry, 57*, 285–295.